IEEE Photonics Journal
An IEEE Photonics Society Publication

Open Access

Analogue of Electromagnetically Induced Transparency in an S-Shaped All-Dielectric Metasurface

Volume 11, Number 3, June 2019

Jinyan Diao
Bingxin Han
Jie Yin
Xiangjun Li
Tingting Lang
Zhi Hong

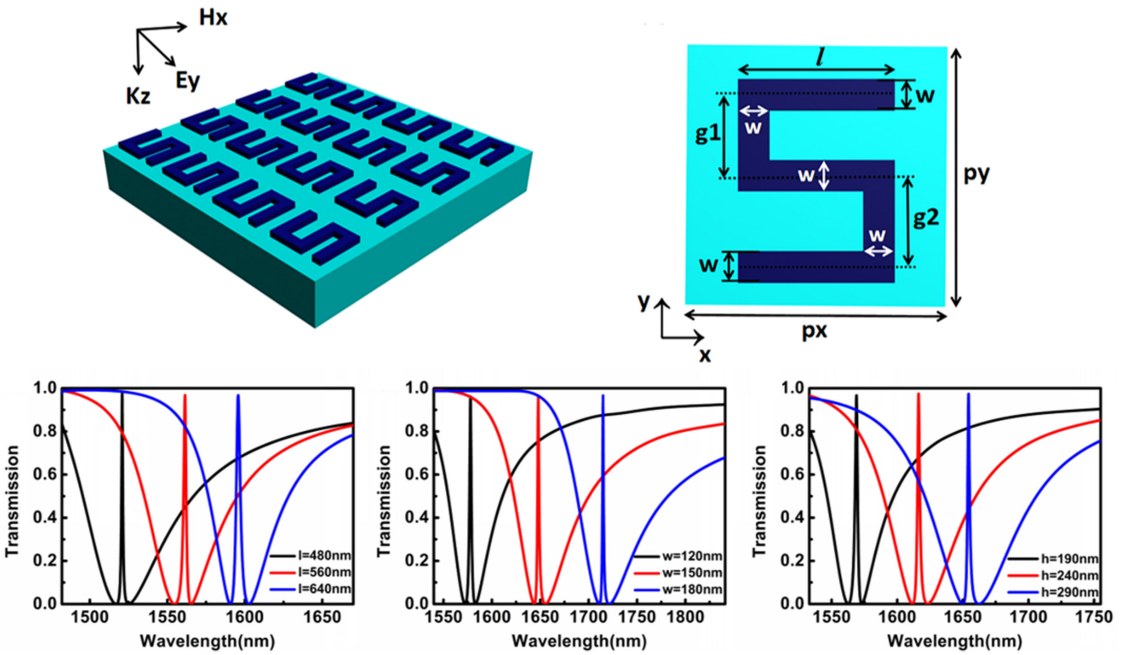

DOI: 10.1109/JPHOT.2019.2920433
1943-0655

Analogue of Electromagnetically Induced Transparency in an S-Shaped All-Dielectric Metasurface

Jinyan Diao, Bingxin Han, Jie Yin, Xiangjun Li, Tingting Lang, and Zhi Hong

Centre for THz Research, China Jiliang University, Hangzhou 310018, China

DOI:10.1109/JPHOT.2019.2920433

Manuscript received April 4, 2019; revised May 15, 2019; accepted May 28, 2019. Date of publication June 3, 2019; date of current version June 14, 2019. This work was supported in part by the National Natural Science Foundation of China (NSFC) under Grant 61875179 and Grant 61875251.
Corresponding author: Zhi Hong (e-mail: hongzhi@cjlu.edu.cn).

Abstract: We proposed and numerically investigated an analogue of electromagnetically induced transparency (EIT) all-dielectric metasurface that features one asymmetric *S*-shaped silicon resonator in the unit cell and generates high transparency, high *Q*-factor resonance in the near infrared spectral region. Breaking the symmetry of the *S*-shaped structure could provide a pathway to excite a trapped magnetic mode that coupled to a bright electric dipolar moment, achieving a sharp EIT-like response. And the *Q* value of the resonance can be easily modified by altering the asymmetric degree of the structure. In particular, the transparency window will almost maintain its symmetric shape and high transmission of 97%, but shift accordingly as the structural parameters (silicon bar's length, width, or thickness) vary in a large range, because of the very small detuning between the two coupled modes. The proposed *S*-shaped all-dielectric metasurface could ease fabrication challenges and have potential applications in biochemical sensing, narrowband filters, optical modulations, and slow light devices.

Index Terms: Electromagnetically induced transparency, all-dielectric metasurface, high Q-factor

1. Introduction

Electromagnetically induced transparency (EIT) is a quantum destructive interference effect that occurs in three energy atomic levels, resulting in a narrow transparency window in the original absorption spectrum [1]–[4]. It was subsequently demonstrated in plasmonic metamaterials [5]–[12]. Because the highly dispersive and the transparent nature of the atomic medium can be drastically modified in the transparency window, it was widely used in the slow-light devices [5], [6], [9], [12], optical sensors [13], [14], and enhancing nonlinearity [15]. But plasmonic metasurfaces showed extremely large bandwidth resonances at infrared and optical frequencies on account of ohmic loss, severely limiting the achieve of high transparency, high Q-factor and large group index [5], [8], [12]. Recently, new strategies in view of the EIT or Fano resonances based on all-dielectric metasurfaces were introduced to restrain these losses, which have exhibited great possibility of producing high Q-factor resonances [16]–[32]. A common feature of the EIT-like all-dielectric metasurface demonstrated so far is dependent on multiple interacted structures within the unit cell, such as orthogonal silicon bars [25]–[27], silicon-based bar-ring resonator [28]–[30]. Generally in these

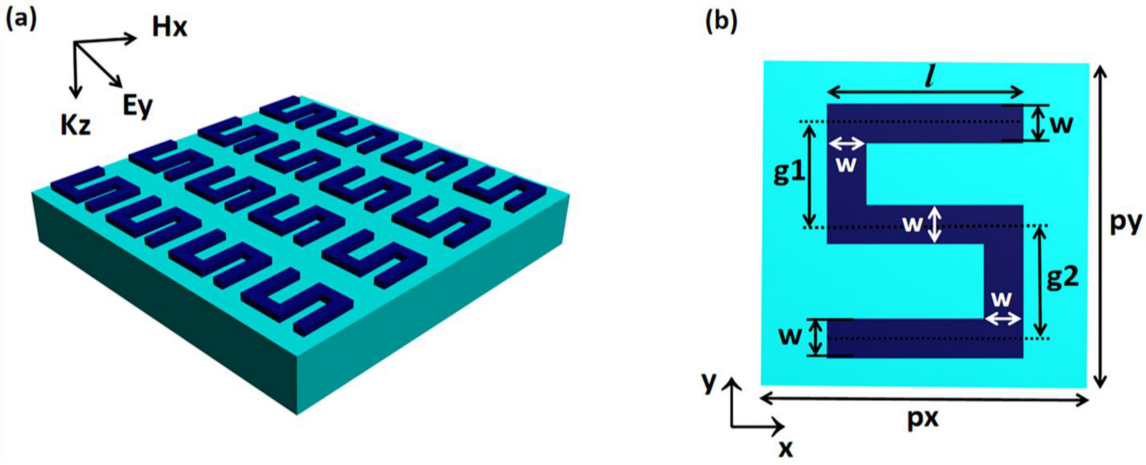

Fig. 1. (a) Schematic of an S-shaped all-dielectric metasurface. (b) Unit cell of the metasurface.

resonator systems, one structure is designed to support the bright mode that can directly couple to the free space, the other one is served as a dark or trapped mode, which is less-accessible, or inaccessible from the incident optical field. By proper design, they can interfere resulting in a high transparency EIT-like window. It should be noted that the EIT-like response can be considered as a special form of Fano line-shape resonance under certain conditions including the small detuning and different Q-values between the two coupled modes [33]. Meanwhile, metasurfaces consisting of single asymmetric structure usually produce Fano resonances, because the detuning between the two interacted modes is not easy to adjust [20], [32], [34]–[36]. Furthermore, as far as the articles currently reported, it is difficult for the resonant frequency of the bright mode to keep the same pace with that of the dark mode when multiple parameters of the structure vary in a large range, which will result in a large detuning between the two coupled modes and make the EIT-like transparency window changed into asymmetric Fano resonance [25]–[32]. And it should be mentioned that the EIT-like response also can be realized in metamaterial waveguide by coupling between a low Q dipolar resonance and a high Q guided mode resonance (GMR). But it is known that the GMR based EIT-like resonance is sensitive to variations in structural parameters as well [37]–[41].

In this article, we proposed and numerically demonstrated an asymmetric S-shaped all-dielectric metasurface that achieves EIT-like response. Simulation results show that the presented asymmetric S-shaped metasurface can support a trapped magnetic mode that couples to a bright electric resonance, producing high transparency, high Q-factor EIT-like resonance. Furthermore, the EIT-like resonance will shift accordingly as the structural parameters of bar's length, width and thickness change, but the symmetric shape of the EIT-like transparency window will almost not be affected owing to the small detuning between the two interacted modes. Such an EIT-like all-dielectric metasurface may ease fabrication challenges and have potential applications in bio-chemical sensing, optical switching, storage of quantum information and low-loss slow-light devices.

2. Design and Simulation Results

2.1 Structure of S-Shaped Silicon Metasurface

The proposed all-dielectric metasurface consists of an S-shaped silicon array (refractive index $n = 3.7$) with a thickness $h = 200$ nm, which is deposited on a quartz substrate ($n = 1.48$), as shown schematically in Fig. 1(a). Each unit cell of the metasurface depicted in Fig. 1(b) comprises three parallel and two vertical connected silicon bars, the geometrical dimensions are as follows: $l = 600$ nm, $w = 120$ nm, $g1 + g2 = 660$ nm, Δg is defined as $\Delta g = g2\text{-}g1$ and $\Delta g \neq 0$ means the S-shaped structure is asymmetric. The structure is periodically arranged in the x-y plane with a same lattice constant of $px = py = 1000$ nm. To investigate resonant properties of the system, numerical

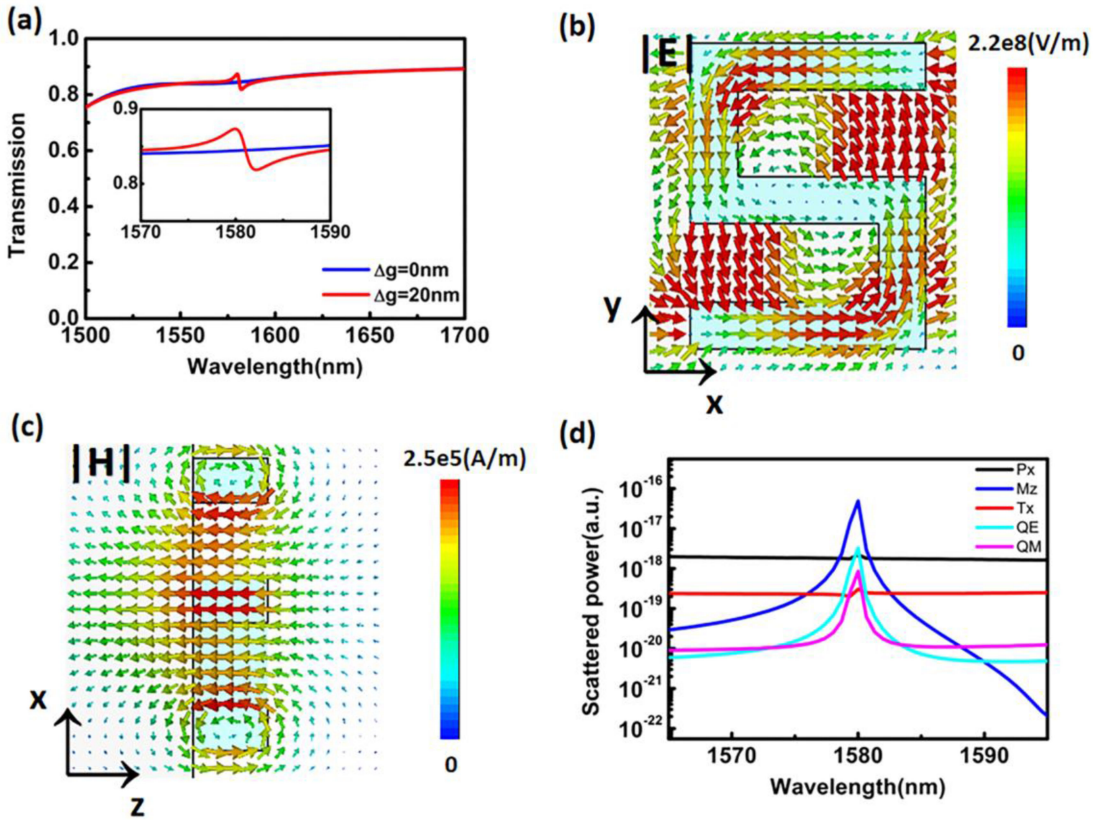

Fig. 2. (a) Transmission spectra of the symmetric S-shaped metasurface ($\Delta g = 0$ nm) and asymmetric S-shaped metasurface ($\Delta g = 20$ nm) when the E-field of incident wave is along the *x*-axis. (b), (c) Distributions of the electric in the *x*-*y* plane and the magnetic in the *x*-*z* plane at $\lambda = 1580$ nm, respectively. (d) The multipole decomposition results of the scattering spectrum by using the Cartesian coordinate system for asymmetric S-shaped metasurface, where *Px*, *Mz*, *Tx*, *QE* and *QM* are the electric dipole in *x*-direction, magnetic dipole in *z*-direction, toroidal dipole in *x*-direction, electric quadrupole and magnetic quadrupole, respectively. The log scale of *y*-axis is chosen in order to display more clearly the contribution results of the multipole decomposition.

simulations of the structure are carried out by commercial CST software. In our simulations, we utilize periodic boundary conditions in both *x* and *y* directions and perfectly matched layers (PMLs) are applied in the wave propagating direction *z*. The structure is illuminated by a plane wave that polarized along the *x*-axis or *y*-axis at normal incidence. And a semi-infinite quartz substrate is assumed in our simulation, thus the GMRs induced by MM waveguides can be excluded.

2.2 Trapped Mode in Asymmetric Metasurface

When the E-field of incident wave is along the *x*-axis, the transmissions of the S-shaped metasurface are studied both in symmetric ($\Delta g = 0$ nm) and asymmetric ($\Delta g = 20$ nm) cases and given out in Fig. 2(a). It is obvious that there is no resonances found in the range from 1500 nm to 1700 nm for the symmetric metasurface, meaning that the metasurface cannot be directly excited. However, a narrow resonance can be clearly seen at a wavelength of 1580 nm in the asymmetric structure, which indicates the appearance of the resonance is attributed to the breaking of the symmetry of the structure. As theoretical analysis referred, the origin of the narrow spectral response can be dated back to so-called “trapped mode” which is weakly coupled to the free space [34], [42]. To further study the physical mechanism of this resonance, we primary analyze the electromagnetic fields of different cross sections around 1580 nm, and the distributions of the electric in the *x*-*y*

plane and the magnetic in the *x*-*z* plane are demonstrated in Fig. 2(b) and 2(c), respectively. The circulating electric field can be clearly observed around the S-shaped structure from Fig. 2(b), which is reminiscent of the magnetic dipole field forms. Rather than the ordinary in-plane magnetic dipole, Fig. 2(c) shows that the displacement currents are polarized along the *z*-axis in the center of the structure, corresponding to a *z*-directed magnetic dipole. Meanwhile, we can notice that the circulating magnetic fields locate inside upper and lower bars of the S-shaped structure in Fig. 2(c), meaning that the electric dipole also contributes to this resonance. Thus, through the electromagnetic field patterns, we may not be able to accurately determine the resonant nature of the response.

In order to get deep understand of the resonance around 1580 nm, the Cartesian multipole contributions into the scattered powers for the asymmetric S-shaped all-dielectric metasurface are calculated, which rely on the induced current inside of the metamolecules [43]–[45]. The dominant five scattering powers of multipoles around the resonant wavelength are shown in Fig. 2(d), where *P*, *M*, *T*, *QE* and *QM* are the electric dipole, magnetic dipole, toroidal dipole, electric quadrupole and magnetic quadrupole, respectively. Here, higher order dipoles are ignored because of the extremely smaller intensity on the scattered powers. Above and below the resonant wavelength of $\sim$1580 nm, the electric dipole *Px* occupies the main role, meaning the S-shaped structure is electrically excited. However, in the vicinity of the resonance, the *z*-directed out-plane magnetic dipole, *Mz*, instead of ordinary in-plane *My*, increases remarkably and dominates all other multipole moments by nearly 22 times than the electric dipole *Px* and about 14 times larger than the electric quadrupole *QE*, around 2 orders stronger than the toroidal *Tx*, and $\sim$58 times than the magnetic quadrupole *QM*. It is believed that the high Q-factor of the resonance is owing to the excitation of this out-plane magnetic dipole in the metasurface [20]. Note that a trapped magnetic mode is excited in our asymmetric S-shaped metasurface, rather than a toroidal mode excited in reported E-shaped metasurface [32].

2.3 Analogue of EIT in Asymmetric Metasurface

Upon excitation with an *y*-polarized incident wave, the transmission spectrum of the symmetric S-shaped structure ($\Delta g = 0$ nm) is investigated and shown in Fig. 3(a). A clear broad resonance dip with a low Q-factor of $\sim$29 can be easily seen at a wavelength of 1580 nm. Here, the Q-factor of the resonance can be calculated by form of $Q = \lambda_0 / FWHM$, Where λ_0 is the central wavelength of the resonance, and the *FWHM* is the corresponding full width at half maximum of the resonance. The corresponding E-field in the *x*-*y* plane and M-field in the *x*-*z* plane are demonstrated in Fig. 3(b) and 3(c), respectively. We notice that the opposite direction circular displacement currents are induced simultaneously around the upside and downside of the symmetric S-shaped structure in Fig. 3(b). Each part of them could generate a magnetic field, and the homologous *z*-component magnetic field of upside is along $+z$ axis, and $-z$ axis for downside. These induced magnetic field patterns with different directions will form a circulation in a head-to-tail manner (see Fig. 3(b)), indicating existence of a toroidal dipole moment *T* in *x* direction [46], [47]. At the same time, the circulating magnetic field can be clearly observed in the center of the S-shaped metasurface from Fig. 3(c), demonstrating the electric dipole also contributes to the excitation of this broad resonance. Subsequently, the multipole decomposition is also used to further confirm the properties of this resonance. As given in Fig. 3(d), the contributions of the electric dipole *Py* and the toroidal dipole *Tx* are crossing with each other at 1553 nm, which is far away from the broad resonance dip at a wavelength of 1580 nm. To be specific, before 1553 nm, the toroidal dipole takes the first place and the electric dipole follows closely. While, after 1553 nm, the electric dipole has the largest strength by nearly 3 times than the toroidal dipole, meaning the electric dipole and toroidal dipole both contribute to this resonance, but the electric dipole plays a major role at the resonant dip. It is worth mentioning that the corresponding *y*-component of the electric field dominates all other multipole moments rather than the strong displacement currents along the *x*-direction seen in Fig. 3(b).

However, once the symmetry of S-shaped structure is broken ($\Delta g = 20$ nm), a distinct EIT-like resonance (also shown in Fig. 3(a)) with high transparency about 97% is observed at a wavelength of 1580 nm, the corresponding Q-factor is 800. We can see that the position of the EIT-like transparency

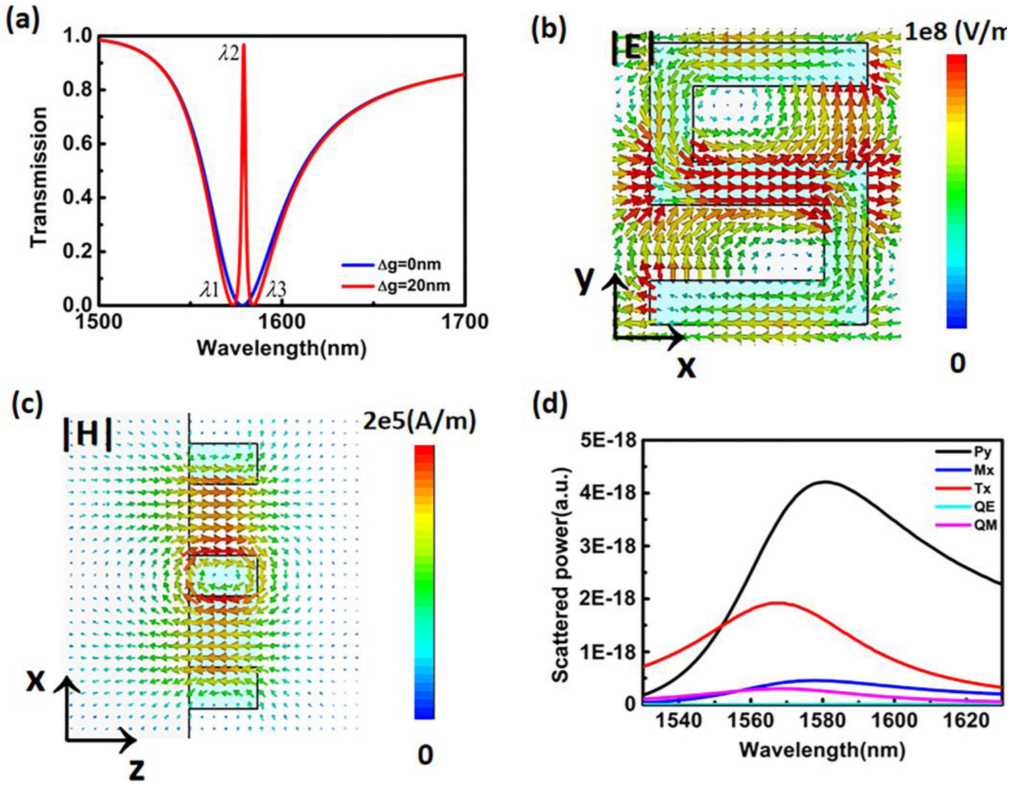

Fig. 3. (a) Transmission spectra of the symmetric S-shaped metasurface ($\Delta g = 0$ nm) and asymmetric S-shaped metasurface ($\Delta g = 20$ nm) when the E-field of incident wave is along the *y*-axis. (b), (c) Distributions of the electric in the *x*-*y* plane and the magnetic in the *x*-*z* plane at $\lambda = 1580$ nm, respectively. (d) The multipole decomposition results of the scattering spectrum by using the Cartesian coordinate system for symmetric S-shaped metasurface, where *Py*, *Mx*, *Tx*, *QE* and *QM* are the electric dipole in *y*-direction, magnetic dipole in *x*-direction, toroidal dipole in *x*-direction, electric quadrupole and magnetic quadrupole, respectively. The log scale of *y*-axis is chosen in order to display more clearly the contribution results of the multipole decomposition.

window coincidentally appears around the dip of the broad electric resonance mentioned above in Fig. 3(a), and it is also consistent with the trapped magnetic resonance given in Fig. 2(a) under the *x*-polarized incident wave. Consequently, the EIT-like resonance can be clearly interpreted by destructive interference between the bright electric dipolar moment and the trapped magnetic dipolar mode, this is different from the reported E-shaped metasurface [32], in which the EIT-like response was achieved by optical coupling between a dark toroidal dipole and a bright magnetic resonance. And breaking the symmetry of the metasurface offers a pathway to excite the trapped magnetic mode [27], [48]. It is worth noting that the EIT-like response can also be achieved by breaking the symmetry of the S-shaped metasurface through changing the length of structural upper or lower horizontal bar.

To better understand the mechanism of the EIT-like response in the asymmetric metasurface, the E-field and M-field plots of the EIT-like transparency window at different wavelengths (dip $\lambda 1$, peak $\lambda 2$, dip $\lambda 3$) are depicted in Fig. 4(a)–4(f), respectively. At the two resonant dips, we can observe that the electromagnetic fields largely focus on the upper and the lower parts of the S-shaped structure. Specifically, there are clear circular displacement currents around the upside of the structure at dip $\lambda 1$ and downside at dip $\lambda 3$ (see Fig. 4(a), 4(c)). Meanwhile, the corresponding magnetic fields locate the upper and lower sides of the structure in Fig. 4(d) and 4(f). Thus, these field modes verify the excitation of the magnetic resonances [21], which can be interpreted by the hybridization method [19], [25], [48], [49]. According to the hybridization model, when the symmetry

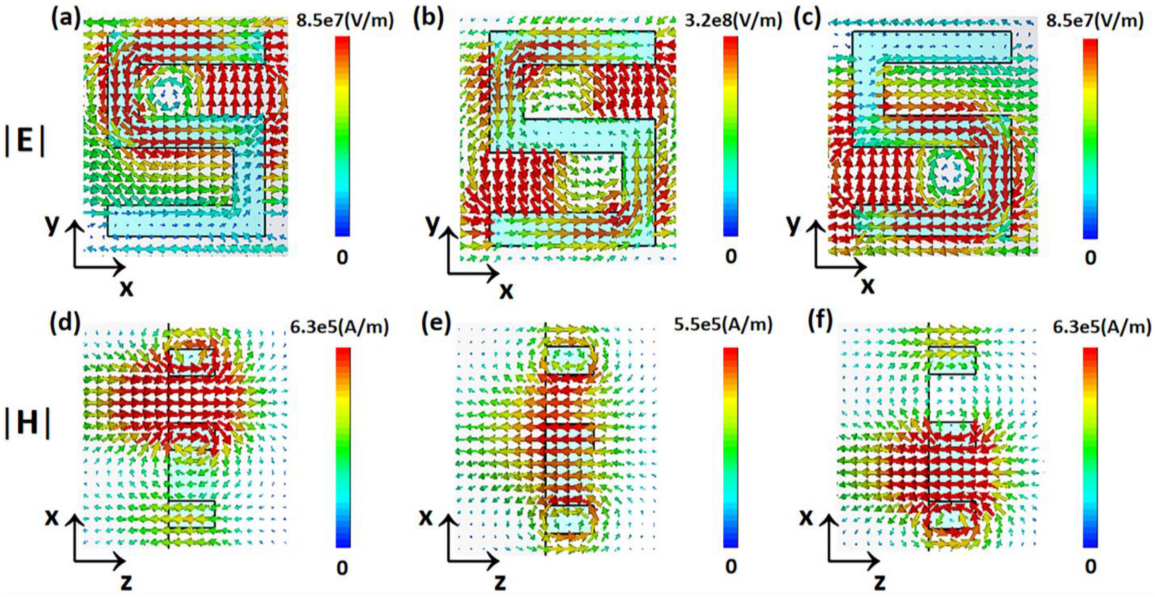

Fig. 4. (a)–(c) The distributions of the electric in the *x-y* plane. (d)–(f) The distributions of the magnetic in the *x-z* plane. (a), (d) dip $\lambda 1$ (1574 nm); (b), (e) peak $\lambda 2$ (1580 nm); (c), (f) dip $\lambda 3$ (1585 nm), respectively.

of the S-shaped metasurface is broken, the hybridization between the bright electric mode and trapped magnetic mode produces the bonding and antibonding modes, which are presented as two resonant dips (dip $\lambda 1$ and dip $\lambda 3$) in the EIT-like transparency window. To be intuitive, the electromagnetic fields in the dip$\lambda 1$ are obtained by the sum of the electromagnetic fields of the bright mode and the trapped mode, which makes the electromagnetic fields focused on the upper part of the S-shaped metasurface. While at the dip $\lambda 3$, the electromagnetic fields mainly distributed in the lower part of the S-shaped are as a result of the electromagnetic fields of the bright mode minus those of the trapped mode. For the transmission peak $\lambda 2$, however, the displacement currents form loops in the E-field and the M-field shows a *z*-directed magnetic dipole, which is consistent with the result in Fig. 2(b)–2(c) and further confirms the excitation of the trapped magnetic mode. So the results of Fig. 4 further verified that the EIT-like response is achieved by a destructive interference between the bright electric mode and the trapped magnetic mode.

2.4 Influence of Structural Parameters on EIT-Like Resonance

At first, considering that the EIT-like response in S-shaped metasurface is mainly determined by the asymmetric degree Δg of the structure, the transmission curves of the metasurface with different values of Δg are calculated, as given in Fig. 5. As Δg decreases from 50 nm to 10 nm, we can see that the EIT-like resonance becomes narrower on account of the decrease of coupling between the bright electric mode and the trapped magnetic mode [28], resulting in an increasing tendency of the Q-factor, and the corresponding Q-factor is 135 for $\Delta g = 50$ nm, and 335 for $\Delta g = 30$ nm, but rising quickly to 3000 when $\Delta g = 10$ nm. Whereas the transmission of the EIT-like response always remains about a high level of 97%.

Moreover, the other geometrical parameters of the metasurface, such as silicon bar's length, width, or thickness will also affect the EIT-like response and presented in Fig. 6. We should mention that the EIT-like resonance considered as a special form of Fano line-shape resonance depends on the degree of detuning between the two coupled modes, which is mainly related to the line width of the bright mode in our case. The EIT-like resonance will have a larger tolerance of the detuning

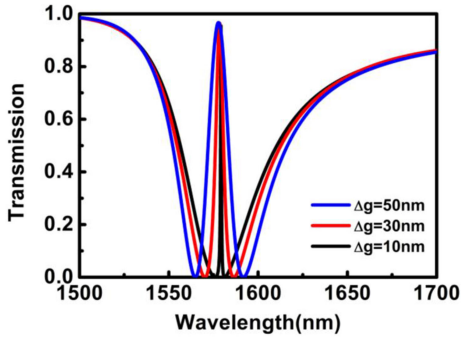

Fig. 5. Transmission spectra of asymmetric S-shaped metasurface with different values of Δg.

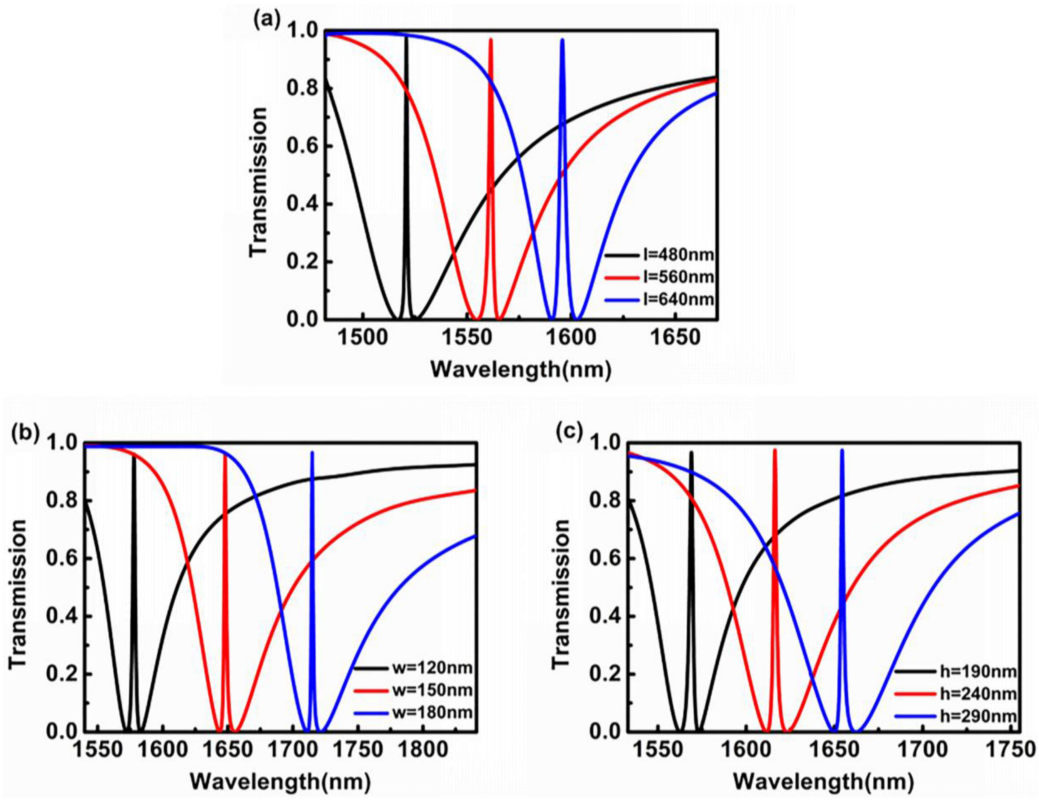

Fig. 6. Transmission spectra of asymmetric S-shaped metasurface ($\Delta g = 20$ nm) with different lengths of l (a), widths of w (b), thicknesses of h (c), respectively.

for a broader bright mode, and if the detuning is over this tolerance, the Fano resonance arises. Here, considering the line width of the trapped mode in our structure is much smaller than that of the bright mode, we define the detuning tolerance of the two coupled modes is about 4% (4 nm) of the line width of the bright mode, corresponding to the Fano index $F = 0.2$, which is defined by Fano formula [33]:

$$I \propto \frac{(F\gamma + \omega - \omega_0)^2}{(\omega - \omega_0)^2 + \gamma^2}$$

Where γ and ω_0 represent the width and position of the resonance. As the length of the silicon bar *l* increases from 480 nm to 640 nm while the rest of geometrical parameters remain the same as depicted in Fig. 1(b), an apparent red shift of the EIT-like transparency window is observed from Fig. 6(a). To be specific, the resonant frequency of the bright electric mode almost keeps the same pace with that of the trapped magnetic mode as the bar length changes, which indicates that the detuning between the two couple modes is very small ($\leq$4 nm), hence, the symmetric shape of the EIT-like resonance is maintained. At the same time, the transmission of the EIT-like response always keeps a high value of 97%, which is very useful for its real applications. Fig. 6(b) presents the transmission spectra of the metasurface calculated at different bar width *w*. In this case, the width varies from 120 nm to 180 nm while the other parameters keep unchanged as well. There is also a noticeable red-shift of the EIT-like resonances with growing *w*, but the shape of the EIT-like transparency windows will not be influenced and the transmission holds a stable level of 97%. Quite similar results can be obtained as above, when the bar thickness *h* ranges from 190 nm to 290 nm, the wavelength of the EIT-like resonance will shift from 1568 nm to 1655 nm, as shown in Fig. 6(c), and the EIT-like responses keep a stable high transmission all the time. However, as far as the articles currently reported, the EIT-like response of MMs is only insensitive to variations in partial parameters of structure, for example, the EIT-like transparency window in E-shaped metasurface is only insensitive to the length of horizontal silicon bar [32], but the detuning of the two interacted modes will become larger than the tolerance as other structural parameters change, including bar's width or vertical bar's length. And similar results can be seen in silicon-based bar-ring resonator [28], of which the EIT-like response is only insensitive to the thickness of the structure, but is very sensitive to variations in the other structural parameters (ring's radius, bar's length, or bar's width).

For all cases up to here, we can reveal that the presented S-shaped metasurface has achieved robust, high Q-factor and high transparency EIT-like resonance when the structural parameters *l*, *w*, and *h* vary over a wide range, which will greatly ease fabrication challenges. Keep in mind that the condition of $g1 + g2 = 660$ nm is important for the metasurface to achieve the EIT-like response, otherwise the resonant wavelength of the bright electric mode cannot keep the same pace with that of the trapped magnetic mode, resulting in large detuning between the two interacted modes and thereafter asymmetric Fano resonance arises.

3. Conclusion

In summary, we have presented and numerically investigated the EIT-like responses in an asymmetric S-shaped all-dielectric metasurface in the near infrared spectral region. A high transparency window and high Q-factor EIT-like resonance is achieved by the destructive interference between the bright electric dipolar moment and the trapped magnetic dipolar mode through the asymmetric structure. And it is worth mentioning that the out-plane trapped magnetic mode is excited and verified by the Cartesian multipole expansion. Meanwhile, the bandwidth of the transparency window can be easily designed by modifying the asymmetric degree of the structure. In particular, the EIT-like transparency window will shift accordingly as the structural parameters(silicon bar's length, width, or thickness) change in a wide range, but the symmetric shape of the EIT-like responses will almost not be affected and the transmission of the EIT-like resonances keeps a stable value of 97%. It is expected that the proposed S-shaped EIT-like all-dielectric metasurface could ease the fabrication challenges and have wide applications in bio-chemical sensing, optical switching and slow-light devices.

References

[1] K. J. Boller, A. Imamolu, and S. E. Harris, "Observation of electromagnetically induced transparency," *Phys. Rev. Lett.*, vol. 66, no. 20, pp. 2593–2596, 1991.
[2] S. E. Harris, "Electromagnetically induced transparency," *Phys. Today*, vol. 50, no. 7, pp. 36–42, 1997.
[3] C. L. Garrido Alzar, M. A. G. Martinez, and P. Nussenzveig, "Classical analog of electromagnetically induced transparency," *Amer. J. Phys.*, vol. 70, no. 1, pp. 37–41, 2002.

[4] M. Fleischhauer, A. Imamoglu, and J. P. Marangos, "Electromagnetically induced transparency: Optics in coherent media," *Rev. Mod. Phys.*, vol. 77, no. 2, pp. 633–673, 2005.
[5] S. Zhang, D. A. Genov, Y. Wang, M. Liu, and X. Zhang, "Plasmon-induced transparency in metamaterials," *Phys. Rev. Lett.*, vol. 101, 2008, Art. no. 047401.
[6] N. Papasimakis, V. A. Fedotov, N. I. Zheludev, and S. L. Prosvirnin, "Metamaterial analog of electromagnetically induced transparency," *Phys. Rev. Lett.*, vol. 101, 2008, Art. no. 253903.
[7] N. Verellen *et al.*, "Fano resonances in individual coherent plasmonic nanocavities," *Nano Lett.*, vol. 9, no. 4, pp. 1663–1667, 2009.
[8] R. Singh, C. Rockstuhl, F. Lederer, and W. Zhang, "Coupling between a dark and a bright eigenmode in a terahertz metamaterial," *Phys. Rev. B*, vol. 79, 2009, Art. no. 085111.
[9] P. Tassin, L. Zhang, T. Koschny, E. N. Economou, and C. M. Soukoulis, "Low-loss metamaterials based on classical electromagnetically induced transparency," *Phys. Rev. Lett.*, vol. 102, 2009, Art. no. 053901.
[10] N. Liu *et al.*, "Plasmonic analogue of electromagnetically induced transparency at the Drude damping limit," *Nature Mater.*, vol. 8, no. 9, pp. 758–762, 2009.
[11] X. Liu *et al.*, "Electromagnetically induced transparency in terahertz plasmonic metamaterials via dual excitation pathways of the dark mode," *Appl. Phys. Lett.*, vol. 100, 2012, Art. no. 131101.
[12] J. Gu *et al.*, "Active control of electromagnetically induced transparency analogue in terahertz metamaterials," *Nature Commun.*, vol. 3, 2012, Art. no. 1151.
[13] N. Liu *et al.*, "Planar metamaterial analogue of electromagnetically induced transparency for plasmonic sensing," *Nano Lett.*, vol. 10, no. 4, pp. 1103–1107, 2010.
[14] Z. G. Dong *et al.*, "Enhanced sensing performance by the plasmonic analog of electromagnetically induced transparency in active metamaterials," *Appl. Phys. Lett.*, vol. 97, 2010, Art. no. 114101.
[15] Y. Sun *et al.*, "Electromagnetic diode based on nonlinear electromagnetically induced transparency in metamaterials," *Appl. Phys. Lett.*, vol. 103, 2013, Art. no. 091904.
[16] J. Groep and A. Polman, "Designing dielectric resonators on substrates: Combining magnetic and electric resonances," *Opt. Exp.*, vol. 21, no. 22, pp. 26285–26302, 2013.
[17] C. Wu *et al.*, "Spectrally selective chiral silicon metasurfaces based on infrared Fano resonances," *Nature Commun.*, vol. 5, 2014, Art. no. 3892.
[18] Y. Yang *et al.*, "Nonlinear Fano-resonant dielectric metasurfaces," *Nano Lett.*, vol. 15, no. 11, pp. 7388–7393, 2015.
[19] W. Zhao, X. Leng, and Y. Jiang, "Fano resonance in all-dielectric binary nanodisk array realizing optical filter with efficient linewidth tuning," *Opt. Exp.*, vol. 23, no. 5, pp. 6858–6866, 2015.
[20] S. Campione *et al.*, "Broken symmetry dielectric resonators for high quality factor Fano metasurfaces," *ACS Photon.*, vol. 3, no. 12, pp. 2362–2367, 2016.
[21] J. A. Schuller, R. Zia, T. Taubner, and M. L. Brongersma, "Dielectric metamaterials based on electric and magnetic resonances of silicon carbide particles," *Phys. Rev. Lett.*, vol. 99, 2007, Art. no. 107401.
[22] Q. Zhao, J. Zhou, F. Zhang, and D. Lippens, "Mie resonance-based dielectric metamaterials," *Mater. Today*, vol. 12, no. 12, pp. 60–69, 2009.
[23] S. Jahani and Z. Jacob, "All-dielectric metamaterials," *Nanotechnology*, vol. 11, pp. 23–36, 2016.
[24] J. Zhang, W. Liu, Z. Zhu, X. Yuan, and S. Qin, "Strong field enhancement and light-matter interactions with all-dielectric metamaterials based on split bar resonators," *Opt. Exp.*, vol. 22, no. 25, pp. 30889–30898, 2014.
[25] F. Zhang, Q. Zhao, J. Zhou, and S. Wang, "Polarization and incidence insensitive dielectric electromagnetically induced transparency metamaterial," *Opt. Exp.*, vol. 21, no. 17, pp. 19675–19680, 2013.
[26] J. Zhang, W. Liu, X. Yuan, and S. Qin, "Electromagnetically induced transparency-like optical responses in all-dielectric metamaterials," *J. Opt.*, vol. 16, 2014, Art. no. 125102.
[27] Z. Wei *et al.*, "Analogue electromagnetically induced transparency based on low-loss metamaterial and its application in nanosensor and slow-light device," *Plasmonics*, vol. 12, no. 3, pp. 641–647, 2017.
[28] Y. Yang, I. I. Kravchenko, D. P. Briggs, and J. Valentine, "All-dielectric metasurface analogue of electromagnetically induced transparency," *Nature Commun.*, vol. 5, 2014, Art. no. 5753.
[29] Z. Wang, Q. Lu, Y. Wang, and Q. Huang, "Electromagnetically induced transparency and absorption in a compact silicon ring-bus-ring-bus system," *Opt. Exp.*, vol. 25, no. 13, pp. 14368–14377, 2017.
[30] E. Petronijevic and C. Sibilia, "All-optical tuning of EIT-like dielectric metasurfaces by means of chalcogenide phase change materials," *Opt. Exp.*, vol. 24, no. 26, pp. 30411–30420, 2016.
[31] L. Zhu, X. Zhao, L. Dong, J. Guo, X. J. He, and Z. M. Yao, "Polarization-independent and angle-insensitive electromagnetically induced transparent (EIT) metamaterial based on bi-air-hole dielectric resonators," *RSC Adv.*, vol. 8, no. 48, pp. 27342–27348, 2018.
[32] B. Han, X. Li, C. Sui, J. Diao, X. Jing, and Z. Hong, "Analog of electromagnetically induced transparency in an E-shaped all-dielectric metasurface based on toroidal dipolar response," *Opt. Mater. Exp.*, vol. 8, no. 8, pp. 2197–2207, 2018.
[33] B. L. Yanchuk *et al.*, "The Fano resonance in plasmonic nanostructures and metamaterials," *Nature Mater.*, vol. 9, no. 9, pp. 707–715, 2010.
[34] V. A. Fedotov, M. Rose, S. L. Prosvirnin, N. Papasimakis, and N. I. Zheludev, "Sharp trapped-mode resonances in planar metamaterials with a broken structural symmetry," *Phys. Rev. Lett.*, vol. 99, 2007, Art. no. 147401.
[35] W. Cao, R. Singh, I. A. I. Al-Naib, and M. He, A. J. Taylor, and W. Zhang, "Low-loss ultra-high-Q dark mode plasmonic Fano metamaterials," *Opt. Lett.*, vol. 37, no. 16, pp. 3366–3368, 2012.
[36] G. Liu *et al.*, "A high-performance refractive index sensor based on Fano resonance in Si split-ring metasurface," *Plasmonics*, vol. 13, no. 1, pp. 15–19, 2018.
[37] Y. Sun, H. Chen, X. Li, and Z. Hong, "Electromagnetically induced transparency in planar metamaterials based on guided mode resonance," *Opt. Commun.*, vol. 392, pp. 142–146, 2017.
[38] H. Chen, J. Liu, and Z. Hong, "Guided mode resonance with extremely high Q-factors in terahertz metamaterials," *Opt. Commun.*, vol. 383, pp. 508–512, 2017.

[39] C. Sui, B. Han, T. Lang, X. Li, X. Jing, and Z. Hong, "Electromagnetically induced transparency in an all-dielectric metamaterial-waveguide with large group index," *IEEE Photon. J.*, vol. 9, no. 5, Oct. 2017, Art. no. 4600708.
[40] Y. Ding and R. Magnusson, "Doubly-resonant single-layer bandpass optical filters," *Opt. Lett.*, vol. 29, no. 10, pp. 1135–1137, 2004.
[41] Y. Ding and R. Magnusson, "Resonant leaky-mode spectral-band engineering and device applications," *Opt. Exp.*, vol. 12, no. 23, pp. 5661–5674, 2004.
[42] S. Prosvirnin and S. Zouhdi, "Resonances of closed modes in thin arrays of complex particles," in *Advances in Electromagnetics of Complex Media and Metamaterials*, S. Zouhdi, A. Sihvola, and M. Arsalane, Eds. Dordrecht, The Netherlands: Kluwer, 2003, pp. 281–290.
[43] E. E. Radescu and G. Vaman, "Exact calculation of the angular momentum loss, recoil force, and radiation intensity for an arbitrary source in terms of electric, magnetic, and toroid multipoles," *Phys. Rev. E*, vol. 65, 2002, Art. no. 046609.
[44] V. Savinov, V. A. Fedotov, and N. I. Zheludev, "Toroidal dipolar excitation and macroscopic electromagnetic properties of metamaterials," *Phys. Rev. B*, vol. 89, 2014, Art. no. 205112.
[45] A. A. Basharin *et al.*, "Dielectric metamaterials with toroidal dipolar response," *Phys. Rev. X*, vol. 5, 2015. Art. no. 011036.
[46] K. Marinov, A. D. Boardman, V. A. Fedotov, and N. Zheludev, "Toroidal metamaterial," *New J. Phys.*, vol. 9, 2007, Art. no. 324.
[47] T. Kaelberer, V. A. Fedotov, N. Papasimakis, D. P. Tsai, and N. I. Zheludev, "Toroidal dipolar response in a metamaterial," *Science*, vol. 330, no. 6010, pp. 1510–1512, 2010.
[48] J. He, J. Wang, P. Ding, C. Fan, and E. Liang, "Gain-assisted plasmon induced transparency in T-shaped metamaterials for slow light," *J. Opt.*, vol. 17, 2015, Art. no. 055002.
[49] E. Prodan, C. Radloff, N. J. Halas, and P. Nordlander, "A hybridization model for the plasmon response of complex nanostructures," *Science*, vol. 302, no. 5644, pp. 419–422, 2003.